



Geochemical characteristics of weathering crusts on the Dzhezhimparma Ridge and the Nemskaya Upland (South Timan)

Oksana V. Grakova✉, Nataliya Yu. Nikulova, Yuliya S. Simakova

Institute of Geology FRC Komi SC of the Ural Branch of the RAS, Syktyvkar, Russia

How to cite this article: Grakova O.V., Nikulova N.Yu., Simakova Yu.S. Geochemical characteristics of weathering crusts on the Dzhezhimparma Ridge and the Nemskaya Upland (South Timan). *Journal of Mining Institute*. 2025. Vol. 272. N 16405, p. 3-15.

Abstract

Numerous local varieties of weathering crusts are known in the South Timan. They differ in their position in the section, type of weathering products, substrates, and occurrence. The aim of the research is to identify patterns in the distribution of rock-forming, rare and rare earth elements and the composition of clay minerals in clay formations of the weathering crusts. The main task is to describe the occurrence and geochemical features that enable determining the genetic type and formation conditions of weathering crusts. The paper presents the results of a study of the distribution of petrogenic, rare earth, rare elements, and clay minerals in weathering crust of different ages, genetic types and occurrence conditions on the Dzhezhimparma Ridge and the Nemskaya Upland in the South Timan. We found that hydromica-kaolinite-type weathering crust is developed after the Late Riphean Dzhezhim Fm. rocks in the basement-cover contact zone on the Dzhezhimparma Upland, and the layer of fine-grained rock at the base of the Devonian section previously considered a weathering crust was formed as a result of mechanical destruction of the Devonian sandstones during movement in the thrust zone. In the Vadyavozh quarry located on the Nemskaya Upland, we studied and described the formations of Mesozoic-Cenozoic areal and linear weathering crusts after the Late Riphean Dzhezhim Fm. rocks. We found that micaceous siltstones in the siltstone-sandstone strata of the Dzhezhim Fm. are associated with the Riphean stage of crust formation and are composed of weathering crust material redeposited in the epicontinental basin.

Keywords

weathering crust; Dzhezhim Formation; suitesandstones; chemical composition; detrital material; sedimentation conditions; South Timan

Funding

The work was carried out under the State assignment for research of the Institute of Geology FRC Komi SC of the Ural Branch of the RAS: “Deep structure, geodynamic evolution, interaction of geospheres, magmatism, metamorphism, and isotope geochronology of the Timan-Northern Urals segment of the lithosphere”, 122040600012-2; “Sedimentary formations: matter, sedimentation, lithogenesis, geochemistry, lithogenesis indicators, sedimentation reconstruction”, 122040600013-9; “Fundamental issues of mineralogy and mineral formation, minerals as indicators of petro- and ore genesis, mineralogy of ore regions and deposits of the Timan-Northern Urals region and Arctic areas”, 122040600009-2.

Received: 11.03.2024

Accepted: 07.11.2024

Online: 06.03.2025

Published: 25.04.2025

Introduction

Commercial deposits of bauxite, titanium ores, gold and diamond occurrences, etc. are associated with weathering crusts in Timan [1-3]. In the Northern Urals, the redistribution and accumulation of ore components, in particular nickel, occurred in weathering crusts of hyperbasites of the Serov-Mauk ophiolite belt [4]. The enrichment of zircon in rare metal and rare earth elements (REE) from the granitoids of the Chukotka plutonic belt [5] and the formation of REE minerals in the Lower Proterozoic metamorphic schists of the Svalbard Archipelago [6] are associated with endogenous processes and hydrothermal alterations. Ancient Early Riphean weathering crusts (secondary quartzites) in the southern part of the Baltic (Fennoscandian) Shield preceded the rapakivi granite formation, 1.65 Ga [7].



In plain South Timan with a developed Quaternary cover, the Paleozoic and Mesozoic-Cenozoic weathering crusts are penetrated by coring boreholes^{1,2,3}. They are recorded on the day surface only within the few projections of the Riphean basement (Fig.1, *a*), where their distribution area coincides with the outcrops of arkosic sandstones of the Upper Riphean Dzhezhim Fm. [8, 9]. It should be noted that recent studies report on the discovery of a macrofossil assemblage in the Dzhezhim Fm. rocks, which may attribute the age of the Dzhezhim Fm. to Late Vendian [10-12]. However, since the Interdepartmental Stratigraphic Committee has not made any changes to the current stratigraphic chart, we use the stratigraphic subdivision adopted in the existing geological maps [13, 14].

In the South Timan, numerous local varieties of weathering crusts found by drilling during geological survey differ in their position in the section, type of weathering products, substrates, and occurrences. For example, residual weathering crusts are developed after the substrate of terrigenous Late Riphean and Vendian deposits. They have either areal or linear distribution. Weathering crusts redeposited after carbonate rocks of the Yshkemes and Vapol Fms. are present in the composition of clayey-sandy rocks in karst depressions of the pre-Paleozoic topography and basal horizons of the Asyvvozh and Izyamel Fms. Meso-Cenozoic weathering crusts after the Dzhezhim Fm. substrate are represented by both areal (Vadyavozh and Dzhezhim quarries) and linear ones, associated with the Late Jurassic fault tectonics (Vadyavozh quarry). The discovery in 1998 of diamond crystals in the gritstone-sandstone strata of the Devonian section base in the immediate vicinity of weathering crusts exposed to the day surface in the Asyvvozh¹ quarry area in the basement-cover contact zone predetermined the further studies conducted in South Timan [15-18]. The weathering crusts and the basal part of the Devonian section were considered as promising targets in the search for diamond placers of the so-called Vishera type [19].

Over twenty years that passed since the recent studies, the technical capabilities and instrumentation have advanced, allowing the study of targets promising for placer deposits and clay raw materials at a qualitatively new level. New artificial outcrops are made in the operating quarries, penetrating the weathering crusts. Geochemical study of weathering crusts is necessary for paleogeographical reconstructions, unveiling the development history and sedimentation patterns in a poorly studied potentially diamond-bearing region, as well as clarifying the prospects for clay raw materials.

The main objective of the study is to describe the geochemical features, distribution of rock-forming, rare and rare earth elements, and the mineral composition of clay rocks considered to be weathering crust formations.

Research methods and materials

Samples of weathering crusts (11 pcs.) and substrate rocks (4 pcs.) were collected in artificial outcrops of the Asyvvozh and Dzhezhim quarries on the Dzhezhimparma and Vadyavozh ridges of the Nemskaya Upland (Fig.1, *a*). All analytical work was carried out at the Geoscience Collective Use Centre of the Institute of Geology FRC Komi SC of the Ural Branch of the RAS. The rock-forming oxide contents were determined by the traditional gravimetric analysis in the Laboratory of Chemistry of Mineral Raw Materials, maintaining the metrological standards (Conclusion N 774). The contents of rare and rare earth elements were determined on an Agilent 7700x ICP-MS. To transfer the sample into solution, the multi-acid digestion (a mixture of acids in the ratio HNO₃:HF:HCl = 1:5:2) under microwave heating conditions was used. Digestion was carried out in a Sineo MDS-10 microwave digestion system.

¹ Tereshko V.V., Kirillin S.V., Kazantseva G.Ya. et al. Geological survey at 1:50,000 scale in adjacent sheets R-40-73-C,D; R-40-74-C; R-40-85-B; R-40-86-A. Syktyvkar, 1991.

² Kulbakova F.A., Shametko V.G., Torlopova S.M. et al. Prospecting for diamond placers of the Vishera type in the South Timan and southwestern Timan region. Ukhta, 2001.

³ Kirillin S.V., Zharkov V.A., Shumilov A.V. et al. Report on geological survey at 1:200,000 scale in adjacent sheets P-40-XX, P-40-XXVI (Nemskaya area). Syktyvkar, 2002.



The phase composition of rocks was determined using X-ray diffraction analysis of non-oriented and oriented samples subjected to standard diagnostic treatments, by a Haoyuan DX-2700BH X-ray diffractometer, CuK α radiation, 40 kV at 30 mA, scanning interval at $2\theta - 2-70^\circ$, scanning step at $2\theta - 0.05^\circ$, shooting speed – 1 $^\circ/\text{min}$. Semi-quantitative X-ray diffraction analysis of the samples was performed in Profex software.

Brief description of the geological position

The study area is in the southeast of the Timan folded-block structure and is the northeastern part of the Dzhezhim-Ksenofontov megaswell, which formed due to the reverse-thrust displacements and progradation of large block-slices in the Early Jurassic [10]. Such blocks, representing basement projections in which rocks are brought to the surface along a series of thrusts, are the Dzhezhimparma and Vadyavozh anticlinal structures.

The Asyvvozh (I in Fig.1, *a*) and Dzhezhim (II in Fig.1, *a*) quarries are on the Dzhezhimparma ridge, coinciding with the Dzhezhimparma anticlinal structure [13]. In the Asyvvozh quarry (61°47'12" N, 54°06'35" E), weathering crusts are found in the contact zone of the Riphean and

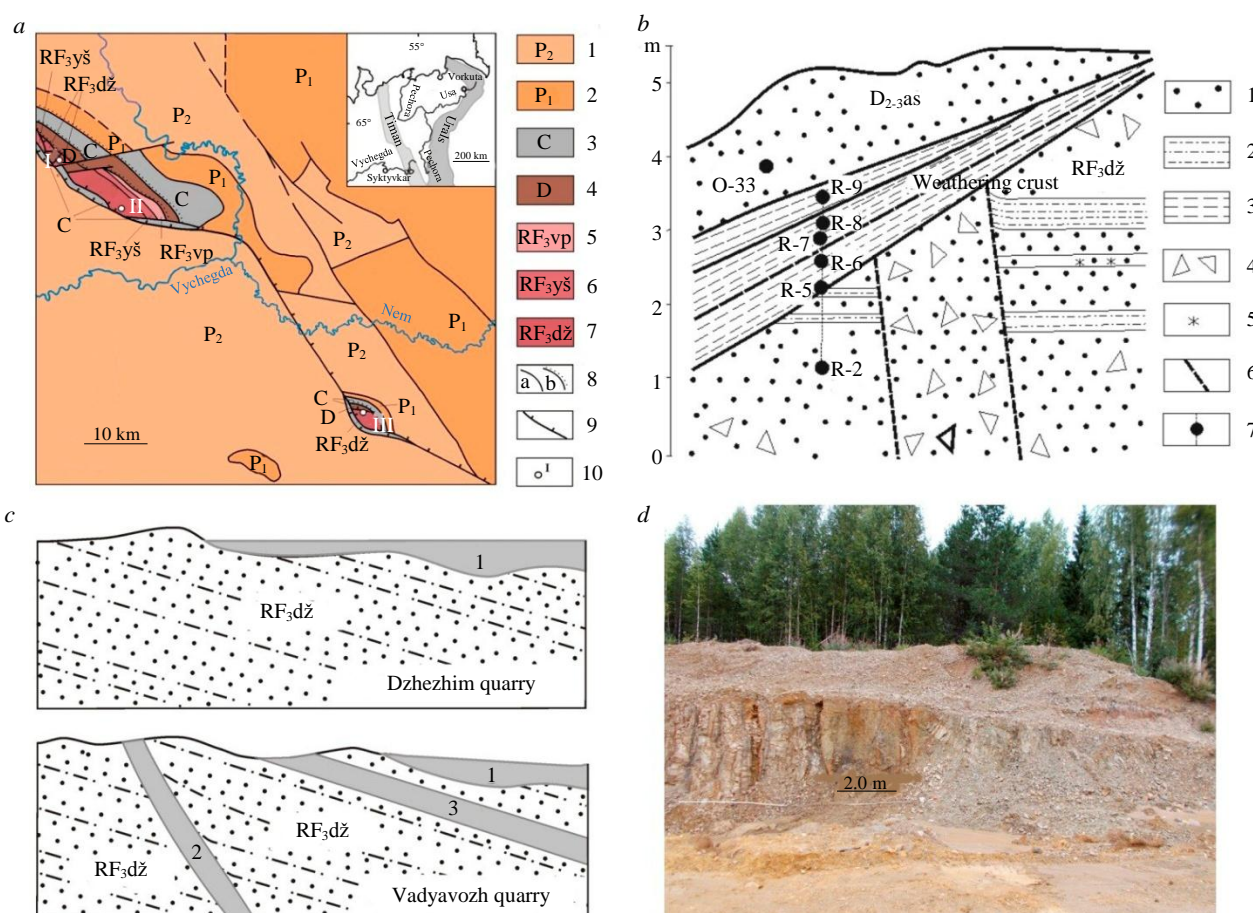


Fig.1. Schematic geological map according to [6]: *a* – 1, 2 – Permian (1 – lower series – limestones, dolomites, siltstones, sandstones, gypsums, 2 – upper series – clays, limestones, sandstones); 3 – Carboniferous – limestones, dolomites, clayey limestones, clays; 4 – Devonian, middle-upper series – gritstones, sandstones, conglomerates, siltstones; 5-7 – Riphean sub-eotheme (5 – Vapol Fm. – dolomites with sandstone, mudstone, and chert interlayers, 6 – Yshkemes Fm. – dolomites, siltstones, mudstones, 7 – Dzhezhim Fm. – sandstones, siltstones, gritstones); 8 – geological boundaries – conformable (*a*), unconformable (*b*); 9 – thrust; 10 – studied sections in quarries (I – Asyvvozh, II – Dzhezhim, III – Vadyavozh); *b* – structural diagram of the section of the contact zone of the Riphean and Devonian deposits in the Asyvvozh quarry: 1 – sandstone; 2 – silty sandstone; 3 – clay; 4 – large-block debris; 5 – ferrugination; 6 – faults; 7 – section line and sampling points; *c* – scheme of the relationship between the Dzhezhim Fm. deposits and weathering crust in the Dzhezhim and Vadyavozh quarries: 1 – Mesozoic-Cenozoic areal; 2 – linear; 3 – weathering crust in the Riphean section; *d* – linear weathering crust after the Dzhezhim Fm. rocks in the Vadyavozh quarry



Paleozoic deposits (Fig.1, *a, b*). The Late Riphean Dzhezhim Fm. (RF_{3dž}) represented by feldspar-quartz sandstones with subordinate interlayers of siltstones and gritstones, lie with an azimuth of 190° SSW and a dip angle of 20-25°. In the contact zone, the Dzhezhim Fm. rocks are disintegrated to a thickness of approximately 10-12 cm and consist of small splintered fragments. The Middle-Late Devonian Asyvvozh Fm. is represented by quartz sandstones with conglomerate, gritstone, siltstone, and clay lenses (dipping azimuth 310° NW and angle 15°). The Precambrian and Paleozoic parts of the section are separated by a wedging-out clay layer, which lies on different layers of the Riphean siltstone-sandstone strata and has a three-membered structure (Fig.1, *b*). In the lower part there is a bed of lilac-pink clayey thin horizontally layered rock with a maximum thickness of about 40 cm (Fig.1, *b*, samples R-5, 6). The bulk clay contains sand-sized grains and rare angular fragments of sandstones, shales, and felsic igneous rocks to 3 cm in size. Above lies a layer (0.5-0.6 m) of pinkish-grey clayey rock similar in structure and texture (Fig.1, *b*, samples R-7 and O-33). It contains single fragments of the above-mentioned rocks to 1.5 cm in size. Directly beneath the base of the Devonian sandstones is a wedging-out layer of greyish-beige sandy-clayey rock to 0.5 m thick (Fig.1, *b, c*, sample R-8). The bulk of this rock contains unevenly distributed coarse sand-sized grains of quartz, isolated fragments of carbonaceous shales and quartz sandstones to 1.5 cm in size. The rock has an obvious external resemblance to the overlying sandstones, lies unconformably on the underlying clays and, in our opinion, could be formed as a result of mechanical destruction of the Devonian rocks. In the geological survey report⁴, clay rocks in this section are classified as linear weathering crusts associated with faults developed after both the Riphean and Devonian rocks. Doubts about this interpretation of the clay rock origin arise from a detailed study of the clay layer structure and its relationship with the underlying rocks (Fig.1, *b*), since hypogene transformations along faults do not cause mechanical redistribution of detrital material and the emergence of thin-layered deposits that lie unconformably on the underlying rocks.

Mesozoic-Cenozoic weathering crusts of the residual areal type, which, according to the geological survey data [14], practically coincide with the Dzhezhim Fm. outcrops of the Upper Riphean, are exposed by the Dzhezhim and Vadyavozh quarries (Fig.1, *a*). In the Dzhezhim quarry (61°42'55" N, 54°21'80" E), the Dzhezhim Fm. is represented by cherry-brown feldspar-quartz sandstones with lenses and interlayers of small-pebble polymictic conglomerates and greyish-brown siltstones. The weathering crust developed after various layers of the Dzhezhim Fm. is expressed by pinkish-grey sandy clay with rare small (to 1.0 cm) fragments of underlying rocks (Fig.1, *d*). The Late Riphean Dzhezhim Fm. exposed by the Vadyavozh quarry (61°27'47" N, 55°49'33" E) is composed of feldspar-quartz sandstones with gritstone, siltstone, and shale interlayers. The Mesozoic-Cenozoic areal residual weathering crust deposits, a few metres thick, in the lower part being the gruss of the original sandstones, siltstones, and shales cemented with clay material, are gradually replaced by a pinkish-yellowish clay mass with an admixture of sand and fragments (to 1.0 cm) of sandstones, siltstones, and shales (Fig.1, *d*). The fact that these crusts were not subject to redeposition is evidenced by the sometimes recognizable relics of the substrate structures⁵. The weathering crusts are covered by a soil and vegetation layer.

Most of the areal weathering crust layer in the Dzhezhim and Vadyavozh quarries was destroyed by previous geological prospecting and modern quarry stone mining. Therefore, the undisturbed weathering crusts are preserved only as individual small outcrops and blocks. The linear weathering crusts that we discovered in the southern wall of the quarry, outside the areal weathering crust zone, where the Riphean rocks are directly overlain by the soil-vegetation layer, are confined to a fault in the Riphean rocks and are represented by a loose olive-brown gruss-sand-clay mixture (Fig.1, *c*). The terrigenous strata of the

⁴ Tereshko V.V., Kirillin S.V., Kazantseva G.Ya. et al. Geological survey at 1:50,000 scale in adjacent sheets R-40-73-C,D; R-40-74-C; R-40-85-B; R-40-86-A. Syktyvkar, 1991.

⁵ Kirillin S.V., Zharkov V.A., Shumilov A.V. et al. Report on geological survey at 1:200,000 scale in adjacent sheets P-40-XX, P-40-XXVI (Nemskaya area). Syktyvkar, 2002.



Dzhezhim Fm. contains interlayers of grey micaceous siltstones that differ significantly from the surrounding rocks (Fig.1, *d*). Analysis of our previous data on the composition and formation conditions of the terrigenous strata in the Vadyavozh quarry [20] allows us to assume the presence of a significant amount of the Riphean intraformational weathering crust material in the fine-grained rocks.

Geochemical characteristics of rocks

The contents of the main rock-forming oxides, lithochemical modules and indicator ratios used to characterize the deposits and reconstruct their formation conditions are given in Table 1. The studied rocks have low alkali content with a noticeable predominance of potassium over sodium and are arkoses (Table 1, Fig.2, *a*) [21]. In the $\log(\text{Fe}_2\text{O}_{3\text{tot}}/\text{K}_2\text{O}) - \log(\text{SiO}_2/\text{Al}_2\text{O}_3)$ diagram [22], the figurative points of the rocks from the Asyvvozh and Vadyavozh quarries are in the arkose and subarkose fields, and the Mesozoic-Cenozoic weathering crust points from the Asyvvozh and Dzhezhim quarries fell into the wacke field (Fig.2, *b*).

Table 1

Chemical composition of rocks (wt.%), indicator ratios, coefficients and modules

Quarry	Asyvvozh							Vadyavozh					Dzhezhim		
Age	RF	Pre-Middle Devonian				D		RF	MZ-KZ		RF (?)		RF	MZ-KZ	
Rock	Sandstone	Redeposited weathering crust				Sandstone	Tectonic clay	Sandstone	Areal weathering crust	Linear weathering crust	Areal weathering crust		Sandstone	Areal weathering crust	
Elements, modules	R-2	R-5	R-6	R-7	R-8	O-33	R-9	V 9.4	V 14.4	V 9.10	V 14.3	V 9.3	Dzh 1	Dzh 2	Dzh 3
SiO ₂	86.2	84.36	75.60	80.64	81.12	86.79	83.52	93.74	86.48	80.48	62.56	62.22	89.80	62.14	69.40
TiO ₂	0.23	0.22	0.50	0.43	0.31	0.34	0.44	0.11	0.26	0.38	0.83	0.71	0.09	0.91	0.62
Al ₂ O ₃	6.57	7.55	11.43	9.50	10.03	7.94	9.04	2.15	6.03	8.90	19.75	17.28	3.59	16.43	13.56
Fe ₂ O ₃	0.42	0.43	2.47	1.14	0.42	0.39	0.47	0.53	1.49	1.78	1.15	3.07	2.22	5.14	3.57
FeO	0.56	0.24	0.24	0.24	0.24	0.14	0.24	1.52	1.34	0.85	0.62	1.68	1.24	0.91	0.88
MnO	0.01	0.01	0.01	0.01	0.01	0.01	0.01	0.02	0.01	0.06	0.01	0.02	0.01	0.03	0.02
MgO	0.26	0.30	0.62	0.46	0.62	0.22	0.46	0.70	0.14	1.02	2.15	3.23	0.15	2.28	1.23
CaO	0.12	0.40	0.40	0.02	0.20	0.26	0.40	0.12	0.23	0.47	0.35	0.47	0.23	0.64	0.70
Na ₂ O	0.24	0.25	0.34	0.28	0.28	0.07	0.09	0.03	0.16	1.35	0.40	0.32	0.56	1.48	2.67
K ₂ O	4.19	4.17	5.14	4.87	4.09	1.39	1.06	0.26	1.52	1.52	6.15	5.21	2.12	4.75	3.67
P ₂ O ₅	0.03	0.05	0.05	0.03	0.04	0.02	0.03	0.05	0.04	0.16	0.05	0.17	0.04	0.13	0.12
LOI	2.03	1.91	2.97	2.11	2.59	2.41	2.41	0.87	2.04	3.01	4.94	5.43	0.67	5.22	3.61
Total	100.90	99.89	99.76	99.73	99.90	99.98	98.20	100.00	99.70	100.00	99.00	99.81	100.70	100.06	100.05
$\log(\text{Na}_2\text{O}/\text{K}_2\text{O})$	-1.24	-1.22	-1.18	-1.24	-1.16	-1.30	-1.07	-0.94	-0.98	-0.05	-1.19	-1.21	-0.58	-0.51	-0.14
$\log(\text{SiO}_2/\text{Al}_2\text{O}_3)$	1.12	1.05	0.82	0.93	0.91	1.04	0.97	1.64	1.16	0.96	0.50	0.56	1.40	0.58	0.71
$\log(\text{Fe}_2\text{O}_{3\text{tot}}/\text{K}_2\text{O})$	-1.00	-0.99	-0.32	-0.63	-0.99	-0.55	-0.35	0.31	-0.01	0.07	-0.73	-0.23	0.02	0.03	-0.01
F1	-3.44	-3.19	-3.53	-3.60	-3.16	-3.71	-3.47	-3.59	-3.51	-1.72	-2.51	-1.68	-3.41	-2.16	-1.12
F2	-4.26	-3.55	-4.01	-3.93	-2.78	0.65	2.22	2.49	-1.11	2.17	-2.59	-0.63	-2.93	-0.29	-0.78
F3	16.13	13.64	8.66	12.04	8.96	0.60	-1.23	-4.10	-1.53	-0.07	5.85	3.70	5.39	3.03	3.52
F4	4.58	3.98	2.51	4.12	3.43	0.56	0.83	5.01	-3.19	-0.08	4.22	4.46	-5.95	2.24	-0.13
K ₂ O/Na ₂ O	17.46	16.68	15.12	17.39	14.61	19.86	11.78	8.67	9.50	1.13	15.38	16.28	3.79	3.21	1.37
SiO ₂ /Al ₂ O ₃	13.12	11.17	6.61	8.49	8.09	10.93	9.24	43.60	14.34	9.04	3.17	3.60	25.01	3.78	5.12
Al ₂ O ₃ /SiO ₂	0.08	0.09	0.15	0.12	0.12	0.09	0.11	0.02	0.07	0.11	0.32	0.28	0.04	0.26	0.20
CIA	56.01	57.13	62.47	62.17	65.59	79.11	81.69	79.63	72.12	65.31	71.25	71.06	49.65	65.24	58.42
CIW	91.46	86.88	89.87	95.03	92.40	93.10	91.16	88.92	89.84	74.31	93.84	92.59	72.82	82.02	70.52



End of Table 1

Quarry	Asyvvozh							Vadyavozh					Dzhezhim		
Age	RF	Pre-Middle Devonian					D	RF	MZ-KZ		RF (?)		RF	MZ-KZ	
Rock	Sandstone	Redeposited weathering crust					Sandstone Tectonic clay	Sandstone	Areal weathering crust	Linear weathering crust	Areal weathering crust		Sandstone	Areal weathering crust	
Elements, modules	R-2	R-5	R-6	R-7	R-8	O-33	R-9	V 9.4	V 14.4	V 9.10	V 14.3	V 9.3	Dzh 1	Dzh 2	Dzh 3
ICV	0.97	0.93	0.93	0.87	0.75	0.42	0.45	1.31	0.66	1.01	0.77	1.05	1.55	1.16	1.17
K ₂ O/Al ₂ O ₃	0.64	0.55	0.45	0.51	0.41	0.18	0.12	0.12	0.25	0.17	0.31	0.30	0.59	0.29	0.27
Na ₂ O+K ₂ O	4.43	4.42	5.48	5.15	4.37	1.46	1.15	0.29	1.68	2.87	6.55	5.53	2.68	6.23	6.34
HM	0.09	0.10	0.19	0.14	0.14	0.10	0.12	0.05	0.11	0.15	0.36	0.37	0.08	0.38	0.27
SPM	0.67	0.59	0.48	0.54	0.44	0.18	0.13	0.13	0.28	0.32	0.33	0.32	0.75	0.38	0.47

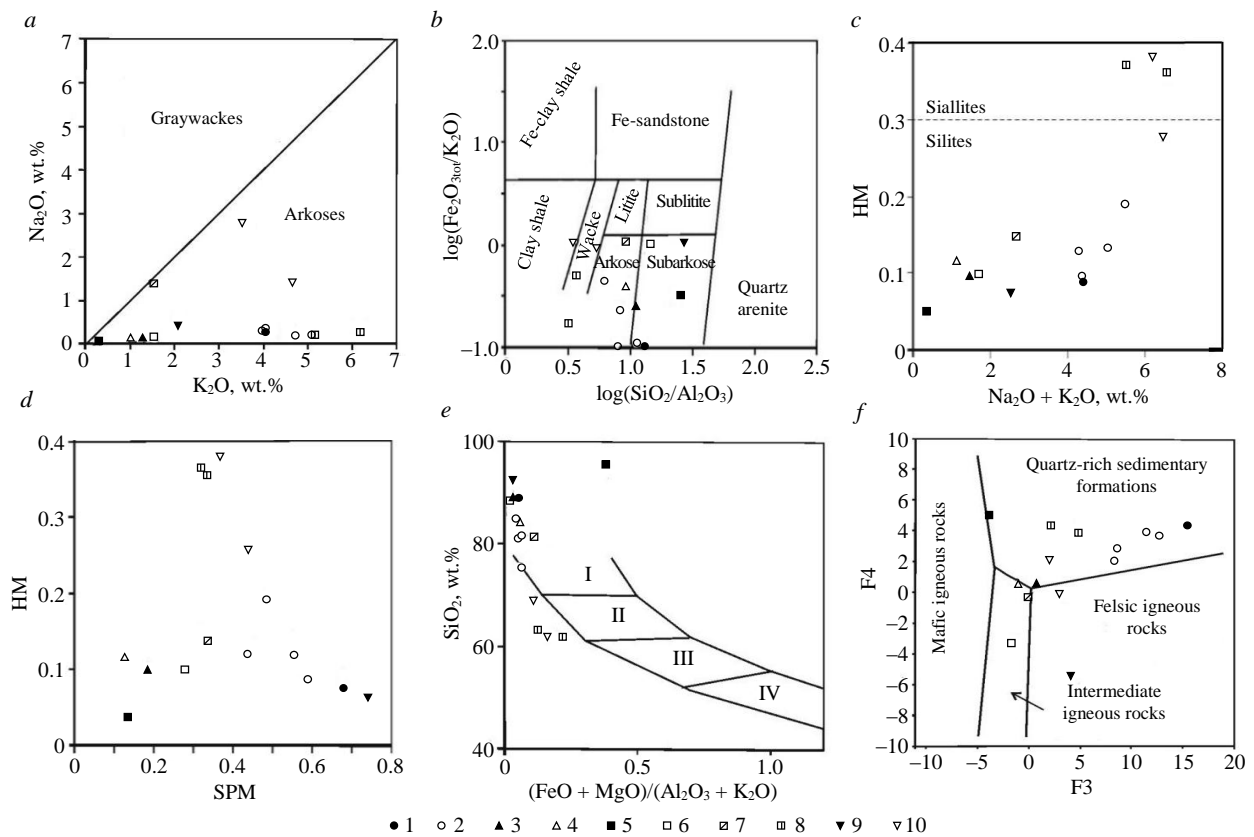


Fig.2. Position of figurative points of rock compositions on classification diagrams: *a* – K₂O – Na₂O [21]; 1-4 – Asyvvozh quarry (1 – sandstone of the Late Riphean Dzhezhim Fm., 2 – weathering crusts after the Dzhezhim Fm. rocks, 3 – sandstone of the Middle-Late Devonian Asyvvozh Fm., 4 – tectonic clay (?); 5-7 – Vadyavozh quarry (5 – sandstone of the Late Riphean Dzhezhim Fm., 6 – areal weathering crusts after the Dzhezhim Fm. rocks, 7 – linear weathering crusts after the Dzhezhim Fm. rocks); 8 – ancient (Riphean) weathering crusts; 9, 10 – Dzhezhim quarry (9 – sandstone of the Late Riphean Dzhezhim Fm., 10 – areal weathering crusts after the Dzhezhim Fm. rocks); *b* – $\log(\text{SiO}_2/\text{Al}_2\text{O}_3) - \log(\text{Fe}_2\text{O}_{3\text{tot}}/\text{K}_2\text{O})$ [22]; *c* – Na₂O+K₂O – HM; *d* – SPM – HM [23]; *e* – $(\text{FeO} + \text{MgO})/(\text{Al}_2\text{O}_3 + \text{K}_2\text{O}) - \text{SiO}_2$: I – rhyolites, granites, II – dacites, granodiorites, III – andesites, diorites, IV – basalts, gabbro [24]; *f* – F₃ – F₄ [25]; *g* – $\text{Fe}_2\text{O}_3 + \text{FeO} - \text{Al}_2\text{O}_3 - \text{CaO} + \text{MgO} + \text{K}_2\text{O} + \text{Na}_2\text{O}$ [26]: 1-3 – correlation fields of weathering products (1 – initial, zone of bleaching and mechanical disintegration, 2 – clayey, clay products of hypogene transformation of rocks, 3 – final, kaolin and bauxite clays, bauxites, iron ores); I-III – correlation fields of igneous rocks (I – ultramafic, II – mafic, III – intermediate and felsic)



After the hydrolyzate module (HM) values in accordance with the classification by Ya.E. Yudovich and M.P. Ketris [24], the substrate rocks and most of the clay formations of the weathering crust are sialites, and the three points corresponding to the samples distinguished by the maximum contents of hydrolyzate elements are siallites – rocks whose alumina content is due to the presence of kaolinite (Fig.2, c). For most of the studied samples, the sodium-potassium module (SPM) value exceeds 0.3 (Fig.2, d), which is a criterion [23] for the presence of unaltered potassium feldspar in the rocks. The Riphean sandstones from the Vadyavozh quarry and the linear weathering crust formations, Devonian sandstones and underlying clays, located in the subarkose field on the classification diagram (Fig.2, a, b) are distinguished by low SPM values (Fig.2, d).

In the $(\text{FeO}+\text{MgO})/(\text{Al}_2\text{O}_3+\text{K}_2\text{O}) - \text{SiO}_2$ diagram [24] showing fragments of various types of igneous rocks in the sediment, most of the figurative points were found to be near the felsic rocks region, and the points of the Mesozoic-Cenozoic areal weathering crusts from the Vadyavozh and Dzhezhim quarries are observed near the field of intermediate rocks (Fig.2, e). In the factor diagram F3 – F4 [25], which considers the ratio of rock-forming oxides, the figurative points corresponding to these samples also gravitate toward the field of igneous rocks of intermediate composition (Fig.2, f). The Devonian sandstones and underlying clays fell into the field formed by igneous rocks of felsic composition (Fig.2, f). The position of most of the figurative points in the diagram of weathering products chemistry [26] allows us to assume that most of the studied rocks contain detrital material inherited from felsic and intermediate igneous rocks that were weakly weathered in arid climate conditions (Fig.2, g).

The chemical index of alteration (CIA) values [27] for the Devonian sandstones and underlying clays, the Mesozoic-Cenozoic and Riphean areal weathering crusts in the Vadyavozh quarry slightly exceed 70 and correspond to warm climate conditions in the erosion area (Table 1). A wide range of the index of compositional variability (ICV) values [28] suggests the presence of detrital material of varying maturity in the rock [22]. For most of the studied samples, the chemical index of weathering (CIW) [21] in the range of 82-95 corresponds to rocks containing weathering crust material (Fig.3, a). In the K/Al – Mg/Al diagram [29], the points of the Riphean sandstones and weathering crusts are in the area of rocks dominated by illite and potassium feldspar. The points of the Devonian sandstones and underlying clays are near the kaolinite trend (Fig.3, b).

According to X-ray diffractometric analysis, the approximate quantitative content of minerals for the studied samples was, %: muscovite (illite) ~ 6-25, chlorite ~ 1-3, smectite ~ 0-15, feldspars ~ 0-10, quartz ~ 20-70. The composition and percentage ratio of finely dispersed component minerals in the samples of different rocks vary. In all the studied samples, the constantly present layered silicate is muscovite of the ordered polytypic structure $2M_1$. A smectite-like mineral (mixed-layer swelling phase) was found in the linear weathering crust samples in the Vadyavozh quarry (Fig.4, a, b). Disordered swelling mixed-layer phases of the illite/smectite and chlorite/smectite types are observed in

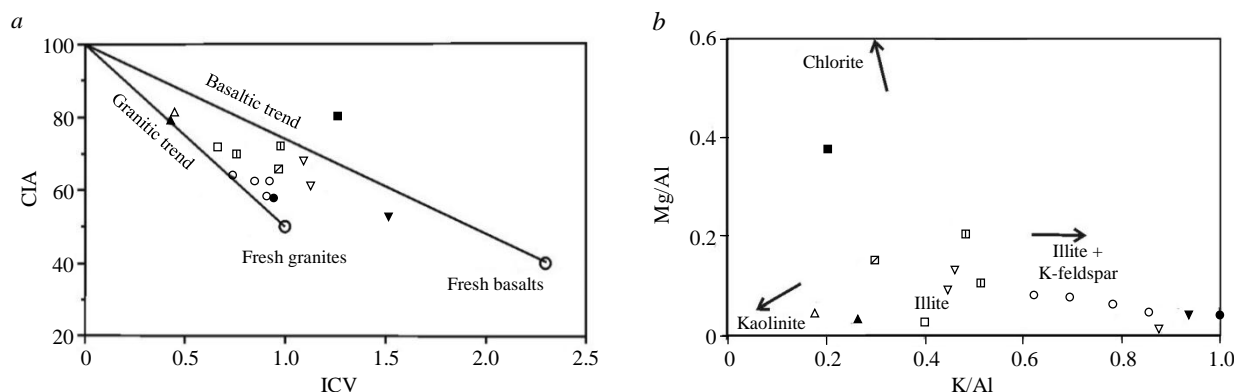


Fig.3. Position of figurative points of rock compositions in diagrams:
 a – ICV – CIA [30]; b – K/Al – Mg/Al [29]. See Fig.2 for legend

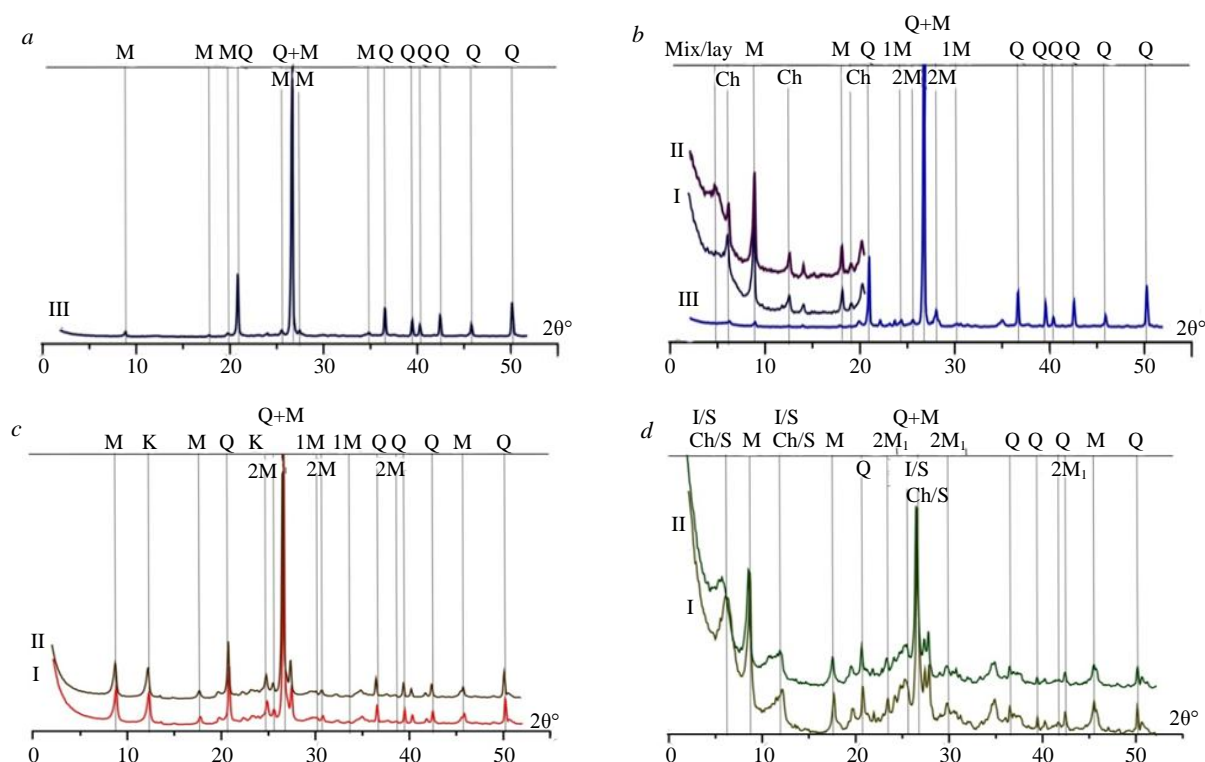


Fig.4. Diffraction patterns of rocks from samples V 14.4 (a), V 9.10 (b), R-8 (c), Dzsh 2 (d)

I – oriented, air-dry; II – oriented, saturated with ethylene glycol; III – non-oriented;
M – muscovite (2M₁ and 1M – polytypic structures); Ch – chlorite; Mix/lay – swelling smectite-like mixed-layer phase;
I/S and Ch/S – disordered mixed-layer illite/smectite and chlorite/smectite formations; K – kaolinite; Q – quartz
See sample numbers in Table 1

the weathering crusts from the Dzhezhim quarry (Fig.4, d). Layered silicates from clays underlying the Devonian sandstones in the Asyvvozh quarry are represented by muscovite and kaolinite (Fig.4, c).

The REE and rare element contents and their ratios used to construct the diagrams and compare them with the Riphean and Devonian rocks are given in Table 2. The total contents of REE in the studied rocks differ insignificantly and are close to the post-Archean Australian shale (PAAS). The highest amounts of REE (263 g/t), including Σ LREE (229 g/t), are observed in sample V 9.3 from the linear weathering crust in the Vadyavozh quarry. The graphs of the REE distribution in sandstones and clay formations of the Asyvvozh quarry are similar to PAAS in the slope of the curves and the europium minimum intensity (Fig.5) [31]. Samples of clayey rocks from the base of the Devonian section (R-9) and Devonian sandstones (O-33) differ from the Riphean sandstones and associated clays in a higher LREE content (Table 2, Fig.5, a) and the absence of a europium minimum (Eu/Eu* 0.90 and 0.92, respectively). The graphs of REE distribution in clayey formations of the Mesozoic-Cenozoic areal weathering crusts from the Dzhezhim quarry are distinguished by a gentle slope in the LREE region [32] compared to the original Riphean sandstones and PAAS and a weak expressed europium minimum (Fig.5, c). The Ce/Ce* ratio of 0.8-1.0 (in sample Dzsh 3 – 0.7) in all studied samples corresponds to the values characteristic of epicontinental settings [33, 34]. In the La/Sc, Zr/Sc, and Th/Sc ratios, the studied rocks are close to the Paleozoic sandstones formed as a result of the destruction of igneous rocks of intermediate and felsic composition [35-37]. The slight excess in the LREE content in sample Dzsh 2 compared to PAAS and the absence of a europium minimum probably reflect increased amount of plagioclase fragments in the composition of the original rocks.

The graphs of REE distribution in clay formations of the weathering crust in the Vadyavozh quarry differ in the nature of the curves slope and the Eu/Eu* ratio. The REE content in them is higher compared to the original Riphean sandstones. Micaceous siltstones (sample V 9.3), attributed to the Riphean weathering crust in the Dzhezhim Fm. (Table 2, Fig.5, c), are distinguished by the maximum



REE content, a steep slope in the LREE region and an intense europium minimum. The studied rocks are close in shape to the upper continental crust (UCC) normalized [38] distribution spectra of trace elements, the content of which in the clay formations of the weathering crust is slightly higher than in the original rocks (Fig.6). The clay formations of the weathering crust are characterized by reduced Co, Ni, Cu, Sr, and Cs contents compared to UCC and increased Zr, Mo, and Pb contents.

Table 2

Content of REE and rare elements, g/t

Quarry	Asyvvozh						Vadyavozh					Dzhezhim		
Age	RF	Pre-Middle Devonian				D	RF	MZ-KZ		RF (?)		RF	MZ-KZ	
Rock	Sandstone	Areal weathering crust				Sandstone Tectonic clay	Sandstone	Areal weathering crust	Linear weathering crust	Areal weathering crust		Sandstone	Areal weathering crust	
Element	R-2	R-5	R-7	R-8	O-33	R-9	V 9.4	V 14.4	V 9.10	V 14.3	V 9.3	Dzh 1	Dzh 2	Dzh 3
Sc	5.5	3.3	4.8	2.0	3.9	5.4	1.0	7.1	5.6	14.0	15.0	1.0	16.0	4.6
V	21.0	21.0	29.0	9.0	16.0	43.0	6.0	45.0	39.0	170.0	119.0	10	110.0	61.0
Cr	26.0	25.0	29.0	11.0	14.0	35.0	204.0	133.0	45.0	137.0	108.0	345.0	114.0	77.0
Co	1.1	0.5	0.5	0.8	1.0	0.6	4.8	4.6	6.6	2.4	11.0	2.5	12.0	10.0
Ni	3.0	2.0	2.0	4.0	6.0	1.0	29.0	20.0	17.0	30.0	42.0	31.0	74.0	51.0
Cu	5.0	6.0	5.0	6.0	7.0	2.0	15.0	45.0	22.0	25.0	24.0	15.0	5.9	7.4
Zn	8.0	5.0	5.0	4.0	10.0	3.0	12.0	16.0	40.0	16.0	39.0	8.3	89.0	50.0
Ga	6.2	6.4	9.6	3.3	5.8	13.0	1.9	10.0	7.2	35.0	24.0	3.9	22.0	14.0
Rb	61.0	62.0	81.0	23.0	37.0	114.0	7.0	61.0	28.0	66.0	93.0	51.0	158.0	41.0
Sr	21.9	27.8	28.9	6.5	8.9	38.0	3.6	12.0	5.5	19.0	12.0	33.0	70.0	46.0
Y	7.9	7.9	10.1	12.0	15.0	14.0	4.1	7.8	6.2	8.8	15.0	7.3	34.0	15.0
Zr	95.0	107.0	147.0	152.0	173.0	189.0	52.0	153.0	62.0	189.0	119.0	38.0	176.0	142.0
Nb	3.2	3.0	4.6	4.7	7.7	6.0	1.2	5.3	2.7	20.0	11.0	1.8	13.0	8.7
Mo	0.9	0.8	0.2	0.2	0.5	0.2	21.0	2.3	0.9	0.8	0.4	4.8	0.5	0.8
Cs	0.9	1.2	2.0	0.8	3.7	2.8	0.1	0.9	0.4	5.3	1.8	0.5	2.3	0.9
La	17.2	19.8	14.7	11.0	17.0	24.0	4.6	22.0	4.5	12.0	51.0	13.0	45.0	12.0
Ce	33.2	40.6	30.7	23.0	35.0	49.0	9.0	43.0	8.1	22.0	111.0	27.0	78.0	19.0
Pr	4.1	5.0	3.8	2.9	4.2	6.4	1.1	4.9	1.2	3.7	12.0	3.5	12.0	3.6
Nd	14.9	19.0	15.0	11.0	15.0	25.0	4.3	18.0	5.0	14.0	46.0	14.0	49.0	14.0
Sm	2.7	3.6	3.0	2.1	2.9	4.8	0.8	3.1	1.3	3.1	8.0	2.5	9.8	3.0
Eu	0.8	1.0	1.0	0.5	0.7	1.5	0.2	0.8	0.3	0.8	1.4	0.9	2.7	12.0
Gd	3.0	3.9	3.9	2.6	3.5	5.1	1.0	3.6	1.4	3.2	8.4	2.6	10.0	3.3
Tb	0.3	0.4	0.4	0.4	0.5	0.6	0.1	0.4	0.2	0.5	0.9	0.3	1.3	0.5
Dy	1.7	1.9	2.1	2.0	2.5	3.0	0.8	1.7	1.2	3.1	3.7	1.4	6.5	2.7
Ho	0.3	0.3	0.4	0.4	0.5	0.6	0.2	0.3	0.2	0.6	0.6	0.3	1.3	0.6
Er	1.0	1.0	1.3	1.3	1.6	1.8	0.5	0.9	0.7	1.8	2.2	0.1	3.7	1.6
Tm	0.1	0.1	0.2	0.2	0.2	0.3	0.1	0.2	0.1	0.3	0.3	0.1	0.5	0.2
Yb	1.0	0.9	1.3	1.3	1.5	1.1	0.4	1.1	0.6	1.8	1.9	0.7	3.1	1.5
Lu	0.2	0.1	0.2	0.2	0.3	0.3	0.1	0.2	1.0	0.3	0.3	0.1	0.5	0.2
Hf	2.9	3.1	4.4	4.2	5.0	5.8	1.4	4.3	1.6	5.3	3.4	1.0	4.9	3.8
W	0.3	0.3	0.3	0.5	0.7	0.3	0.5	0.8	0.5	2.0	0.8	1.6	1.0	0.6
Pb	31.5	130.3	13.8	12.0	23.0	19.0	26.0	51.0	21.0	239.0	70.0	8.3	8.4	3.7
Th	4.9	6.4	5.5	3.7	5.0	8.1	1.7	8.3	3.6	5.8	9.9	2.5	11.0	3.2
U	0.8	1.0	1.1	1.0	1.4	1.5	0.6	2.5	0.7	3.4	3.7	0.7	3.8	0.8
Eu/Eu*	0.9	0.8	0.9	0.7	0.7	0.9	0.6	0.8	0.8	0.7	0.5	1.1	0.8	1.2
Ce/Ce*	0.9	1.0	1.0	0.9	1.0	0.9	0.9	0.9	1.0	0.8	1.1	0.9	0.8	0.7
Σ LREE	73.0	89.0	68.0	51.0	75.0	111.0	20.0	92.0	33.0	56.0	229.0	61.0	197.0	53.0
Σ REE	89.0	106.0	88.0	71.0	101.0	138.0	27.0	108.0	53.0	76.0	263.0	75.0	257.0	78.0

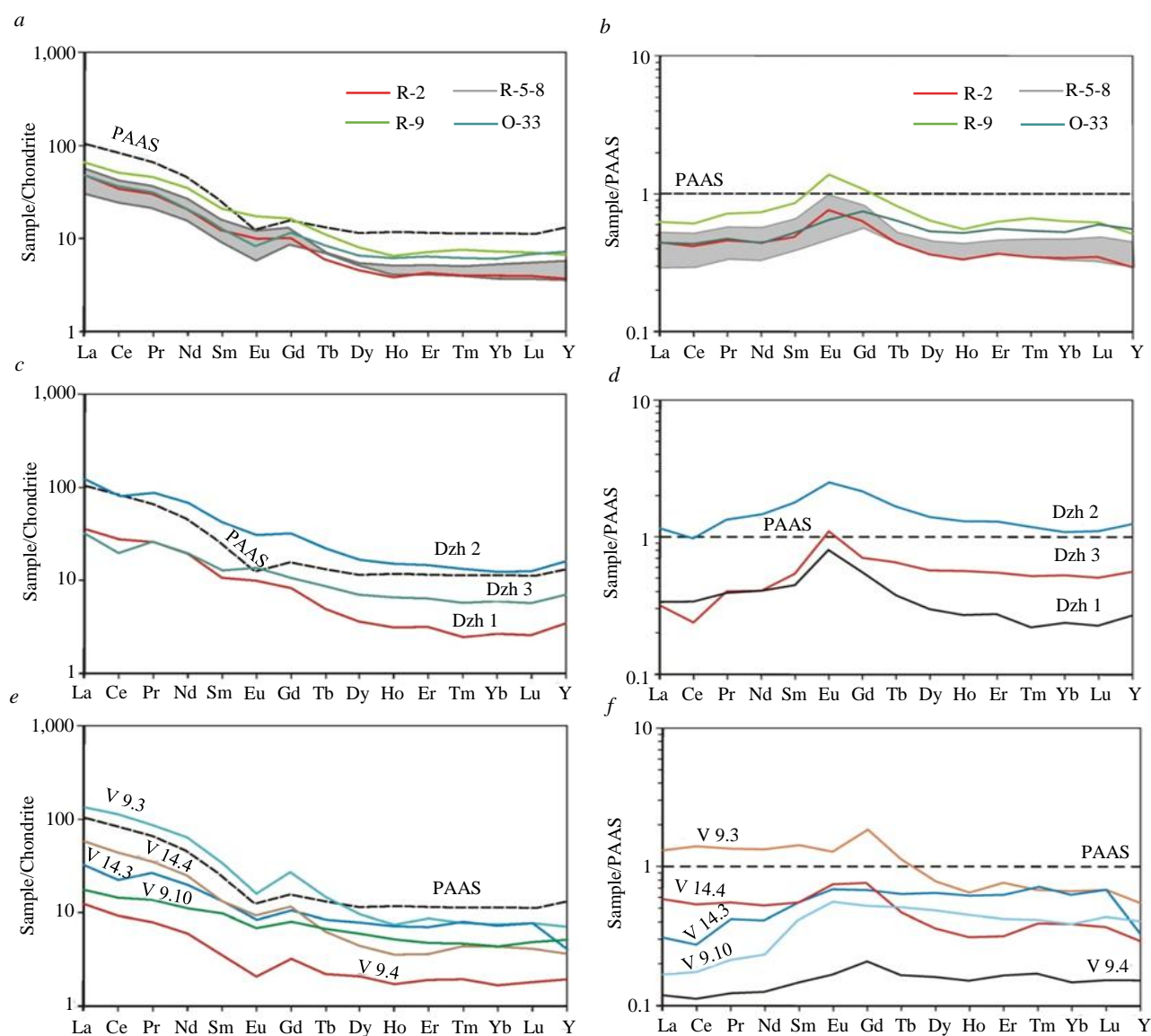


Fig.5. Normalized distribution spectra of REE contents: *a, c, e* – for chondrite [32]; *b, d, f* – for PAAS [31]

Discussion of results and conclusions

The studied varieties of weathering crust in the Riphean rocks differ slightly in the ratio of rock-forming elements, the content and composition of micaceous minerals and are diagnosed as rocks of the bleaching and mechanical disintegration zone. The figurative points of sandstones and clay formations in the $K_2O - Na_2O$ ratio [22], which are arkoses in the $\log(Fe_2O_{3tot}/K_2O) - \log(SiO_2/Al_2O_3)$ diagram (see Fig.2, *b*), are in the field of sub-arkoses and wackes, which includes weathering crust samples distinguished by the highest mica content. The $(Na_2O+K_2O) - HM$ and $SPM - HM$ diagrams [23] show an increase in alkalinity (total and normalized) in samples of weathering crust after the Riphean rocks and a decrease in these parameters for clay formations at the base of the Devonian strata. Devonian sandstones and clays are also distinguished by maximum values of the weathering indices CIA and CIW [21, 27]. The CIW values in the Devonian sandstones and underlying clayey rocks (93 and 91, respectively) characterize them as weathering crust formations. All previous geological surveys and investigations noted the presence of crustal material in the rocks of the Middle-Upper Devonian Asyvvozh Fm. [13, 14] this fact served as an argument for searching for placer diamonds⁶. High CIW values (94 and 93) are also noted in the siltstones of the Dzhezhim Fm., which confirms

⁶ Tereshko V.V., Kirillin S.V., Kazantseva G.Ya. et al. Geological survey at 1:50,000 scale in adjacent sheets R-40-73-C,D; R-40-74-C; R-40-85-B; R-40-86-A. Syktyvkar, 1991.

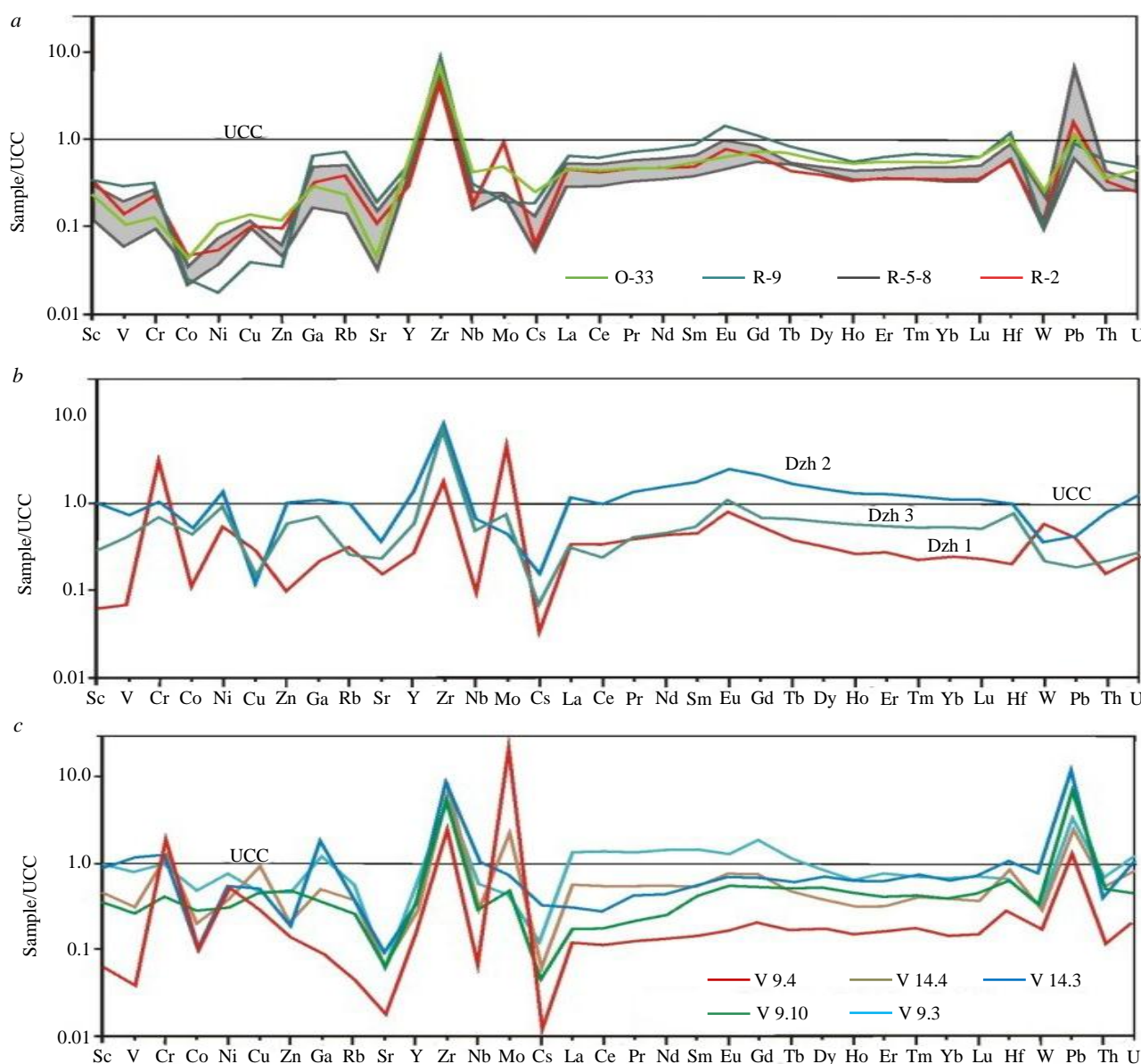


Fig.6. UCC [37] normalized contents of trace elements in the original sandstones and clay rocks

our assumption about their connection with the weathering crust. Riphean sandstones and associated clay formations of the weathering crust from the Asyvvozh quarry contain a significant proportion of feldspars and potassium micas, which, according to the article by Ya.E.Yudovich and co-authors (1991), is characteristic of arid weathering crusts widely developed in the Riphean deposits.

The composition and ratio of clay minerals in multiple-aged weathering crusts differ. The occurrence of disordered swelling mixed-layer formations (illite/smectite, chlorite/smectite) in samples from the Vadyavozh quarry indicates the transformation of the original rocks into weathering crust. A mixed-layer swelling phase was found in the Mesozoic-Cenozoic weathering crust samples. Its content can reach 15 %. In addition to the $2M_1$ structure, they contain a weakly ordered muscovite polytype $1M$, the appearance of which is a diagnostic sign of crust formation. The phase composition of layered silicates in the weathering crust of the Asyvvozh quarry is represented only by muscovite and kaolinite.

In the Asyvvozh quarry, the REE content in the Riphean sandstones and clay formations of the weathering crust differs insignificantly and is close to PAAS. The Devonian sandstones and underlying clays lack a europium minimum. In the Vadyavozh quarry, the micaceous siltstones of the ancient weathering crust in the Dzhezhim Fm. are distinguished by the maximum REE content, a steep slope in the LREE region, and an intense europium minimum (see Table 2, Fig.5, c). In the clays of the



Mesozoic-Cenozoic weathering crust after the Riphean sandstones, the inherited low contents of Co, Ni, Cu, Sr, and Cs compared to UCC and elevated Zr, Mo, and Pb are preserved.

It should be noted that geologists from industrial organizations, during geological survey and exploration, considered the Dzhezhim Fm. deposits and the weathering crusts developed after them as a potential intermediate collector of placer diamonds. The distribution features of rock-forming oxides and REE in the studied weathering crust varieties after the Riphean rocks and in the Riphean psammities themselves do not reveal any signs of kimberlite destruction products [39, 40]. Our studies confirmed the correct identification of siltstones in the Dzhezhim Fm. in the Vadyavozh quarry as rocks formed as a result of the redeposition of the Riphean terrigenous rocks transformed in the weathering crust.

The petrochemical characteristics of the fine-grained rock from the base of the Devonian section and the overlying sandstones are virtually identical. Since the presence of weathering crust material is characteristic of all rocks of the Asyvvoyzh Fm., including those lying where no clay layer is at the strata base in the presence of tectonic contact, we believe that the clay layer formed due to mechanical abrasion of the original sandstones.

REFERENCES

1. Pystin A.M., Glukhov Yu.V., Bushenev A.A. A new diamond find and primary diamond potential of the Chetlas uplift (Middle Timan). *Journal of Mining Institute*. 2023. Vol. 264, p. 842-855.
2. Krasotkina A.O., Skublov S.G., Kuznetsov A.B. et al. First Data on the Age (U–Pb, SHRIMP-II) and Composition of Zircon from the Unique Yarega Oil–Titanium Deposit, South Timan. *Doklady Earth Sciences*. 2020. Vol. 495. Part 2, p. 872-879. DOI: [10.1134/S1028334X20120065](https://doi.org/10.1134/S1028334X20120065)
3. Skublov S.G., Makeyev A.B., Krasotkina A.O. et al. Isotopic and Geochemical Features of Zircon from the Pizhenskoye Titanium Deposit (Middle Timan) as a Reflection of Hydrothermal Processes. *Geochemistry International*. 2022. Vol. 60. N 9, p. 809-829. DOI: [10.1134/S0016702922090063](https://doi.org/10.1134/S0016702922090063)
4. Ilalova R.K., Duryagina A.M., Ageev A.S. Minerogenesis sequence and processes in weathering mantle of ultrabasic rocks of the Serov–Mauk ophiolite belt (Northern Urals). *Mining Informational and Analytical Bulletin*. 2020. N 7, p. 13-26 (in Russian). DOI: [10.25018/0236-1493-2020-7-0-13-26](https://doi.org/10.25018/0236-1493-2020-7-0-13-26)
5. Alekseev V.I., Alekseev I.V. Zircon as a Mineral Indicating the Stage of Granitoid Magmatism at Northern Chukotka, Russia. *Geosciences*. 2020. Vol. 10. Iss. 5. N 194. DOI: [10.3390/geosciences10050194](https://doi.org/10.3390/geosciences10050194)
6. Akbarpuran Haiyati S.A., Gulbin Yu.L., Gembitskaya I.M., Sirotkin A.N. Compositional Evolution of REE- and Ti-Bearing Accessory Minerals in Metamorphic Schists of Atomfjella Series, Western Ny Friesland, Svalbard and Its Petrogenetic Significance. *Geology of Ore Deposits*. 2021. Vol. 63. N 7, p. 634-653. DOI: [10.1134/S1075701521070047](https://doi.org/10.1134/S1075701521070047)
7. Terekhov E.N., Makeyev A.B., Skublov S.G. et al. Quartz Porphyries on the Outer Islands in the Gulf of Finland: Volcanic Comagmates of Rapakivi Granites. *Journal of Volcanology and Seismology*. 2023. Vol. 17. N 6, p. 530-549. DOI: [10.1134/S0742046323700318](https://doi.org/10.1134/S0742046323700318)
8. Kuznetsov N.B., Natapov L.M., Belousova E.A. et al. The first results of U/Pb dating and isotope geochemical studies of detrital zircons from the neoproterozoic sandstones of the Southern Timan (Djejm–Parma Hill). *Doklady Earth Sciences*. 2010. Vol. 435. Part 2, p. 1676-1683. DOI: [10.1134/S1028334X10120263](https://doi.org/10.1134/S1028334X10120263)
9. Latysheva I.V., Kuznetsov N.B., Shatsillo A.V. et al. U–Pb age of detrital zircon grains from clastic rocks of the Dzhezhim Fm. (Upper Precambrian of South Timan). *Geodinamicheskaya evolyutsiya litosfery Tsentralno-Aziatskogo podvizhnogo poyasa (ot okeana k kontinentu): Materialy nauchnoi konferentsii*. Irkutsk: Institut zemnoi kory SO RAN, 2022. Iss. 20, p. 166-169.
10. Kolesnikov A.V., Latysheva I.V., Shatsillo A.V. et al. Ediacara-Type Biota in the Upper Precambrian of the Timan Range (Dzhezhim–Parma Hill, Komi Republic). *Doklady Earth Sciences*. 2023. Vol. 510. Part 1, p. 289-292. DOI: [10.1134/S1028334X23600032](https://doi.org/10.1134/S1028334X23600032)
11. Kolesnikov A.V., Latysheva I.V., Shatsillo A.V. et al. Discovery of Ediacaran-type biota in South Timan. *Geologiya, geoekologiya i resursnyi potentsial Urala i soprodelnykh territorii: Sbornik statei X Vserossiiskoi molodezhnoi konferentsii*. Moscow: Pero, 2022, p. 87-88.
12. Kolesnikov A.V. Stratigraphic correlation potential of the Ediacaran palaeopascichnids. *Estudios Geológicos*. 2019. Vol. 75. N 2. N e102. DOI: [10.3989/egol.43588.557](https://doi.org/10.3989/egol.43588.557)
13. Gosudarstvennaya geologicheskaya karta Rossiiskoi Federatsii. Masshtab 1:1 000 000 (trete pokolenie). Seriya Uralskaya. List R-40 – Severouralsk. Obyasnitelnaya zapiska. St. Petersburg: Kartograficheskaya fabrika VSEGEI, 2005, p. 332.
14. Gosudarstvennaya geologicheskaya karta Rossiiskoi Federatsii. Masshtab 1:200 000. Izdanie vtoroe. Seriya Timanskaya. List R-40-XXVI (Kanava). Obyasnitelnaya zapiska. Moscow: Moskovskii filial FGBU VSEGEI, 2018, p. 105.
15. Grakova O.V. Comparative characteristics and formation conditions of the Devonian diamond-bearing deposits in the South and Middle Timan: Avtoref. dis. ... kand. geol.-mineral. nauk. Syktyvkar: Institut geologii Komi NTs UrO RAN, 2014, p. 19.
16. Grakova O.V., Ulyasheva N.S. Petrographic composition and lithochemical characteristic of diamond-bearing deposit of asyvvoyzh series (D₂₋₃AS) of South Timan. *Vestnik of the Institute of Geology of the Komi Science Center of the Ural Branch of the Russian Academy of Sciences*. 2015. N 12 (252), p. 16-23 (in Russian). DOI: [10.19110/2221-1381-2015-12-16-23](https://doi.org/10.19110/2221-1381-2015-12-16-23)



17. Makeev A.B., Rybalchenko A.Ya., Dudar V.A., Shametko V.G. New prospects for diamond potential in Timan. *Geologiya i mineralnye resursy evropeiskogo severo-vostoka Rossii. Novye rezultaty i novye perspektivy: Materialy XIII Geologicheskogo sezda Respubliki Komi. Syktyvkar*. 1999. Vol. IV, p. 63-66.
18. Tskhadaya N.D., Kobrunov A.I., Shilov L.P. et al. Timan Ridge. In 2 volumes. Vol. 2. Ukhta: Uktinskii gosudarstvennyi tekhnicheskii universitet, 2010, p. 437.
19. Rybalchenko A.Ya., Rybalchenko T.M., Silaev V.I. Theoretical basis for forecasting and exploration of primary diamonds deposits of tuffizit type. *Proceedings of the Komi Science Centre of the Ural Division of the Russian Academy of Sciences*. 2011. Iss. 1 (5), p. 54-66 (in Russian).
20. Nikulova N.Yu. Lithological and chemical composition and depositional conditions of metasediment basement rocks of the Vadyavog prominence (Nem upland, South Timan). *Regional Geology and Metallogeny*. 2017. N 69, p. 23-32 (in Russian).
21. Pettijohn F.J., Potter P.E., Siever R. Sand and sandstone. Moscow: Mir, 1976, p. 535 (in Russian).
22. Herron M.M. Geochemical classification of terrigenous sands and shales from core or log data. *Journal of Sedimentary Research*. 1988. Vol. 58. N 5, p. 820-829. DOI: [10.1306/212F8E77-2B24-11D7-8648000102C1865D](https://doi.org/10.1306/212F8E77-2B24-11D7-8648000102C1865D)
23. Yudovich Ya.E., Ketris M.P. Fundamentals of lithochemistry. St. Petersburg: Nauka, 2000, p. 479.
24. Kusunoki T., Musashino M. Comparison of the Middle Jurassic to Earliest Cretaceous sandstones from the Japanese Islands and South Sikhote-Alin. *Earth Science*. 2001. Vol. 55. Iss. 5, p. 293-306. DOI: [10.15080/agcchikyukagaku.55.5_293](https://doi.org/10.15080/agcchikyukagaku.55.5_293)
25. Roser B.P., Korsch R.J. Determination of Tectonic Setting of Sandstone-Mudstone Suites Using SiO₂ Content and K₂O/Na₂O Ratio. *The Journal of Geology*. 1986. Vol. 94. N 5, p. 635-650.
26. Erofeev W.S., Tsekhovskiy Yu.G. Paragenetic associations of continental deposits (Family of arid parageneses. Evolutionary frequency). Moscow: Nauka, 1983, p. 192 (in Russian).
27. Nesbitt H.W., Young G.M. Early Proterozoic climates and plate motions inferred from major element chemistry of lutites. *Nature*. 1982. Vol. 299. N 5885, p. 715-717. DOI: [10.1038/299715a0](https://doi.org/10.1038/299715a0)
28. Cox R., Lowe D.R. A conceptual review of regional-scale controls on the composition of clastic sediment and the co-evolution of continental blocks and their sedimentary cover. *Journal of Sedimentary Research*. 1995. Vol. 65. N 1a, p. 1-12. DOI: [10.1306/D4268009-2B26-11D7-8648000102C1865D](https://doi.org/10.1306/D4268009-2B26-11D7-8648000102C1865D)
29. Turgeon S., Brumsack H.-J. Anoxic vs dysoxic events reflected in sediment geochemistry during the Cenomanian–Turonian Boundary Event (Cretaceous) in the Umbria–Marche Basin of central Italy. *Chemical Geology*. 2006. Vol. 234. Iss. 3-4, p. 321-339. DOI: [10.1016/j.chemgeo.2006.05.008](https://doi.org/10.1016/j.chemgeo.2006.05.008)
30. Yong Il Lee. Provenance derived from the geochemistry of late Paleozoic–early Mesozoic mudrocks of the Pyeongan Supergroup, Korea. *Sedimentary Geology*. 2002. Vol. 149. Iss. 4, p. 219-235. DOI: [10.1016/S0037-0738\(01\)00174-9](https://doi.org/10.1016/S0037-0738(01)00174-9)
31. Migdisov A.A., Balashov Yu.A., Sharov I.V. et al. Abundance of rare earth elements in the major lithological rock types in the sedimentary cover of the Russian Platform. *Geokhimiya*. 1994. N 6, p. 789-803.
32. Taylor S.R., McLennan S.M. The Continental Crust: Its Composition and Evolution. Moscow: Mir, 1988, p. 312 (in Russian).
33. Murray R.W., Buchholtz Ten Brink M.R., Gerlach D.C. et al. Rare earth, major, and trace elements in chert from the Franciscan Complex and Monterey Group, California: Assessing REE sources to fine-grained marine sediments. *Geochimica et Cosmochimica Acta*. 1991. Vol. 55. Iss. 7, p. 1875-1895. DOI: [10.1016/0016-7037\(91\)90030-9](https://doi.org/10.1016/0016-7037(91)90030-9)
34. Shatrov V.A., Voitsekhovskii G.V. The use of lanthanides for the reconstruction of Phanerozoic and Proterozoic sedimentation environments exemplified by sections in the cover and basement of the East European platform. *Geochemistry International*. 2009. Vol. 47. N 8, p. 758-776. DOI: [10.1134/S0016702909080023](https://doi.org/10.1134/S0016702909080023)
35. Cullers R.L. Implications of elemental concentrations for provenance, redox conditions, and metamorphic studies of shales and limestones near Pueblo, CO, USA. *Chemical Geology*. 2002. Vol. 191. Iss. 4, p. 305-327. DOI: [10.1016/S0009-2541\(02\)00133-X](https://doi.org/10.1016/S0009-2541(02)00133-X)
36. McLennan S.M., Hemming S., McDaniel D.K., Hanson G.N. Geochemical approaches to sedimentation, provenance, and tectonics. *Processes Controlling the Composition of Clastic Sediments*. Geological Society of America, 1993. Special Paper 284, p. 21-40. DOI: [10.1130/SPE284-p21](https://doi.org/10.1130/SPE284-p21)
37. Maslov A.V., Melnichuk O.Yu., Mizens G.A. et al. Provenance reconstructions. Article 2. Litho- and isotope-geochemical approaches and methods. *Lithosphere*. 2020. Vol. 20. N 1, p. 40-62 (in Russian). DOI: [10.24930/1681-9004-2020-20-1-40-62](https://doi.org/10.24930/1681-9004-2020-20-1-40-62)
38. Taylor S.R., McLennan S.M. The geochemical evolution of the continental crust. *Reviews of Geophysics*. 1995. Vol. 33. Iss. 2, p. 241-265. DOI: [10.1029/95RG00262](https://doi.org/10.1029/95RG00262)
39. Gusev N.I., Antonov A.V. Kimberlites of the Serbeyan Prospect (Anabar Shield): melt products enriched with sodium, chlorine, carbonate. *Regional Geology and Metallogeny*. 2020. N 81, p. 105-118 (in Russian).
40. Oparin N.A., Oleinikov O.B. The geology and composition of the Khompu-May field kimberlite pipes (Central Yakutia, Russia). *Arctic and Subarctic Natural Resources*. 2022. Vol. 27. N 4, p. 486-498 (in Russian).

Authors: Oksana V. Grakova, Candidate of Geological and Mineralogical Sciences, Researcher, ovgrakova@geo.komisc.ru, <https://orcid.org/0000-0001-5917-9218> (Institute of Geology FRC Komi SC of the Ural Branch of the RAS, Syktyvkar, Russia), Nataliya Yu. Nikulova, Doctor of Geological and Mineralogical Sciences, Leading Researcher, <https://orcid.org/0000-0002-1511-6124> (Institute of Geology FRC Komi SC of the Ural Branch of the RAS, Syktyvkar, Russia), Yuliya S. Simakova, Candidate of Geological and Mineralogical Sciences, Senior Researcher, <https://orcid.org/0000-0003-0409-4019> (Institute of Geology FRC Komi SC of the Ural Branch of the RAS, Syktyvkar, Russia).

The authors declare no conflict of interests.